



# Tractography for Surgical Neuro-Oncology Planning: Towards a Gold Standard

Sandip S. Panesar<sup>1</sup> · Kumar Abhinav<sup>1</sup> · Fang-Cheng Yeh<sup>2,3</sup> · Timothée Jacquesson<sup>4</sup> · Malie Collins<sup>1</sup> · Juan Fernandez-Miranda<sup>1</sup>

Published online: 12 December 2018  
© The American Society for Experimental NeuroTherapeutics, Inc. 2018

## Abstract

Magnetic resonance imaging tractography permits *in vivo* visualization of white matter structures. Aside from its academic value, tractography has been proven particularly useful to neurosurgeons for preoperative planning. Preoperative tractography permits both qualitative and quantitative analyses of tumor effects upon surrounding white matter, allowing the surgeon to specifically tailor their operative approach. Despite its benefits, there is controversy pertaining to methodology, implementation, and interpretation of results in this context. *High-definition fiber tractography* (HDFT) is one of several non-tensor tractography approaches permitting visualization of crossing white matter trajectories at high resolutions, dispensing with the well-known shortcomings of diffusion tensor imaging (DTI) tractography. In this article, we provide an overview of the advantages of HDFT in a neurosurgical context, derived from our considerable experience implementing the technique for academic and clinical purposes. We highlight nuances of qualitative and quantitative approaches to using HDFT for brain tumor surgery planning, and integration of tractography with complementary operative adjuncts, and consider areas requiring further research.

**Key Words** Tractography · neurosurgical planning · neuro-oncology · white matter anatomy · brain tumors

## Introduction

During the twentieth century, neurosurgical practice underwent several revolutions facilitated primarily by technological advances. Introduction of magnetic resonance imaging (MRI) in the 1980s permitted detailed, noninvasive visualization of neural parenchyma in both normal and pathological conditions. The introduction of diffusion MRI tractography towards the end of the 1990s represented another revolution in neuroimaging as it permitted *in vivo* visualization of white matter fascicular architecture. Prior to its introduction,

knowledge of white matter anatomy and its pathological aberrations was primarily derived from postmortem dissection, animal experiments, and the neurological technique of *aphasiology* [1]. Though these techniques contributed substantially to the neuroanatomical lexicon, each suffered from unique shortcomings [2, 3]. Diffusion MRI tractography addressed many of these by permitting visualization of living white matter over large volumes of healthy and diseased subjects.

Tractography has been adapted for use by neurosurgeons to provide insight into a wide variety of pathologies and for preoperative planning. The latter broadly involves characterizing the spatial characteristics of white matter tracts in relation to lesions, followed by selection of an operative trajectory to avoid these eloquent fibers. Conventional MRI sequences including T1, T2, and fluid-attenuated inversion recovery (FLAIR) can represent locoregional changes in the white matter, for example edema, but cannot differentiate individual white matter pathways. At a qualitative level, tractography therefore allows subjective preoperative visualization of white matter tracts in relation to a space-occupying lesion. Visualizing qualitative changes such as displacement or

---

✉ Juan Fernandez-Miranda  
djfm@stanford.edu

<sup>1</sup> Department of Neurosurgery, Stanford University, 300 Pasteur Drive, Palo Alto, CA 94304, USA

<sup>2</sup> Department of Neurological Surgery, University of Pittsburgh, Pittsburgh, PA, USA

<sup>3</sup> Department of Bioengineering, University of Pittsburgh, Pittsburgh, PA, USA

<sup>4</sup> CHU de Lyon – Hôpital Neurologique et Neurochirurgical Pierre Wertheimer, Lyon, France

disruption of tracts may permit the surgeon to tailor their operative trajectory while minimizing the damage to surrounding fibers. Similarly, these visualized changes, at a simplistic level may be used to prognosticate with the hypothesis that a specific neurologic deficit associated with disruption is potentially irreversible. Quantitative parameters derived from diffusion-weighted MRI sequences, for example fractional anisotropy (FA) or quantitative anisotropy (QA), may also provide further support towards characterizing the nature of change in white matter pathways by lesions like cavernous malformations and tumors (displacement, disruption, infiltration) such as high- and low-grade primary cerebral neoplasms [4–6].

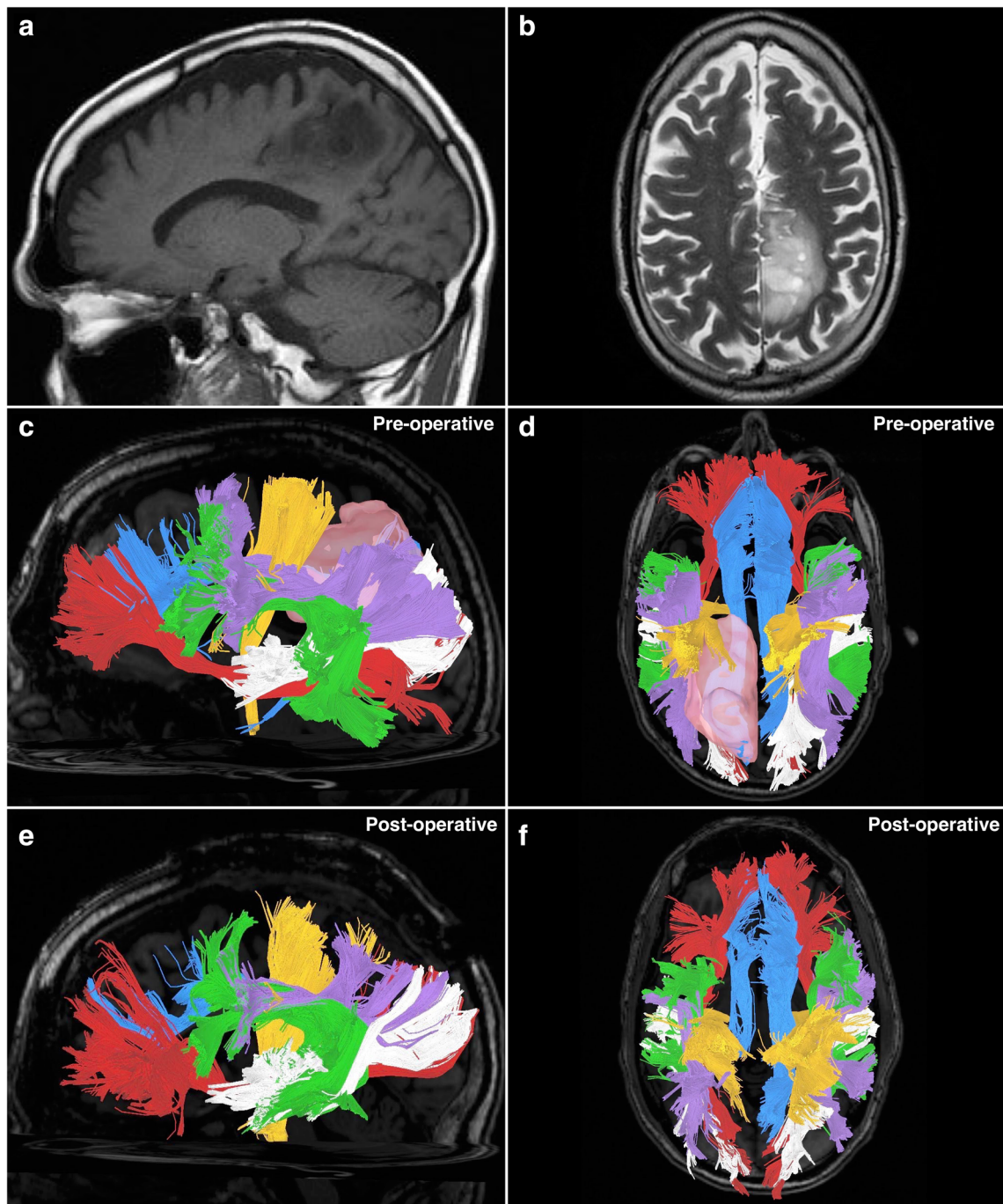
Though diffusion tensor imaging (DTI) [7] was the first and is possibly the most well-known tractography technique, it is known to suffer from several critical shortcomings [8]. Non-tensor tractography approaches have been derived to address these. One of these is high-definition fiber tractography (HDFT). Over the past decade, we have utilized and honed HDFT for preoperative planning in over 100 neurosurgical cases including primary and secondary neoplasms and cavernomas. We have attempted to validate HDFT neuroanatomically [9] and for surgical purposes [10], used it in a series of anatomical studies [11–16], employed it to study quantitative perilesional white matter changes in brain tumors [4, 5] and neurodegenerative conditions [17], and devised a large-volume atlas consisting of averaged diffusion data from over 800 healthy subjects from the Human Connectome Project [18]. We use our extensive experience of HDFT to highlight its benefits for neurosurgical planning, in an effort to increase awareness and implementation among neurosurgeons.

## Methodological Principles

At its most fundamental level, diffusion tractography measures the innate Brownian motion of water molecules confined within axons (anisotropy) by applying multidirectional magnetic resonance sensitizing gradients to neural tissue [19]. The collection of obtained diffusion coefficients is reconstructed by various available tractography algorithms to produce units of directionality corresponding to microstructural white matter orientation in the voxel. Joining a series of these directional units via either deterministic or probabilistic tractography algorithms enables the visualization of *fiber tracts* for study. DTI utilizes at least 6 diffusion gradient samplings to calculate a diffusion tensor, which is a single, averaged unit of directionality [7]. As it employs a Gaussian model, the diffusion tensor is affected by all constituent diffusion coefficients. The tensor therefore has a single primary direction representing the effect of its largest coefficients or would

**Fig. 1** A 66-year-old male was incidentally found to have a left-sided parietal mass following a motor vehicle accident. It was diagnosed as a low-grade glioma and treated expectantly with repeat MRI scans. Twelve years following the diagnosis, he presented with right-sided upper and lower extremity paresthesias and gait instability. It was subsequently biopsied to reveal pathology consistent with anaplastic astrocytoma, World Health Organization (WHO) grade III (IDH mutation, MGMT methylation, TP53 mutation). He subsequently underwent awake craniotomy with tumor resection under image guidance, and awake mapping of the cortex. Postoperative recovery was unremarkable, and the patient was discharged with plans for adjuvant chemotherapy and radiation treatment. **(a)** A preoperative sagittal T1-weighted MRI image demonstrating the parietal lesion on the left. **(b)** A preoperative infero-superior axial T2-weighted MRI image demonstrating the parietal lesion, located adjacent to the sagittal fissure. **(c)** A sagittal image demonstrating preoperatively obtained tractography. The tumor is visible (pink), as are the tracts surrounding it. It is apparent that the tumor has invaded the superior longitudinal fasciculus (purple), which lies atop the arcuate fasciculus (green). Immediately anterior to the tumor is the corticospinal tract (orange). Posterior and inferior to the tumor is the posterior aspect of the middle longitudinal fasciculus (white). Inferior to the tumor is the inferior fronto-occipital fasciculus (red). Behind these tracts lies the cingulum (blue), a para-sagittally oriented tract. **(d)** A superior-aspect axial image demonstrating preoperatively obtained tractography. The tumor is visible (pink), and it is apparent that the tumor has infiltrated a large part of the left posterior cingulum (blue). In close proximity to the tumor are the corticospinal tract (orange) lying anterolaterally, the superior longitudinal fasciculus (purple) running parallel to the tumors lateral margin, and the middle longitudinal fasciculus (white) running inferiorly to the tumors inferior margins. Other visible tracts are the arcuate fasciculus (green) and the inferior fronto-occipital fasciculus (red). If the tracts are compared with the contralateral (right) hemisphere, the effects of displacement and infiltration by the tumor are apparent. **(e)** A sagittal image demonstrating postoperatively obtained tractography. The tumor has been removed. Apparent is that the corticospinal fibers (orange) were previously disrupted by the tumor, as a larger posterior portion is visible following removal, which were not present on the preoperative scan. A portion of the superior longitudinal fasciculus (SLF) which had been infiltrated by tumor has been sacrificed, leaving a thinned-appearing bundle. Otherwise, the other tracts have been largely unaffected from this aspect. **(f)** A superior-aspect axial image demonstrating postoperatively obtained tractography. Following tumor removal, the posterior portion of the left cingulum (blue) has been sacrificed due to tumor infiltration. A larger-appearing left-sided corticospinal tract (orange) and thinner-appearing superior longitudinal fasciculus (purple) are apparent due to displacement and infiltration effects, respectively. The other tracts remain largely unaffected by the procedure

assume a sphere (i.e., perfect isotropy) if coefficient values were equal. It is this fundamental limitation of a single tensor per voxel that renders DTI unable to trace crossing axons at subvoxel resolution produces numerous *false continuities* and prevents the accurate tracking of fibers to their cortical terminations [8, 20–28]. More complex tractographic methods have been devised to address the shortcomings of DTI. HDFT utilizes a non-Gaussian approach, employing generalized Q-sampling imaging (GQI) [29]. GQI is a model-free approach utilizing the Fourier transform relation between the diffusion signals and tissue diffusion displacement. It dispenses with the tensor unit, instead producing a spin distribution function (SDF) corresponding to direction of water diffusion within



the voxel. The SDF is a compound metric, with greater than one element of directionality contributed to by multiple peak diffusion values [30], and can thus address the reproduction of crossing fibers at subvoxel resolutions.

In addition to directional information, DTI and HDFT also provide quantitative indices related to the underlying white matter from which measurements were obtained. The diffusion tensor provides an index of FA [31, 32] in addition to diffusivity [17, 29], both of which are indices of diffusion speed. The SDF provides an index of QA, which is the amount

of anisotropic spins that diffuse along the fiber orientation [29, 33] rather than the velocity of water diffusion. Both FA and QA are used as thresholds to terminate tracking of either probabilistic or deterministic tracking algorithms [17]. Some of the alternative methods to DTI such as high angular resolution diffusion imaging (HARDI) [21] and diffusion spectrum imaging (DSI) [30] utilize a metric known as the orientation distribution function (ODF). Importantly, though these methods are able to visually resolve crossing fibers at subvoxel resolutions, the ODF does not carry radial diffusivity

information [17] and is therefore unable to quantitatively define tissue properties unlike the diffusion tensor or the SDF.

Once the scan data has been reconstructed using either DTI or HDFT methods, each voxel carries a tensor or SDF corresponding to fiber orientation and spin diffusivity properties. In cases of pathology, for example a tumor, differences between the quantitative indices of the intra- or peritumoral voxels and either the contralateral (healthy) hemisphere or the corresponding area in a separate healthy subject may be compared [4, 5, 17]. As this approach involves user-selected regions of interest (ROIs), extensive knowledge of radiological neuroanatomy is necessitated and, due to manual selection of individual tracts, may be subject to significant inter- or intrasubject variability (see “Approaches to Fiber Tracking”). To address this issue, voxel-based analysis approaches involve normalizing serial scans of the same (or different) subjects to a stereotaxic space, for voxel-by-voxel comparison of diffusion differences over time or across subjects [17]. For methods employing more complex diffusion indices such as ODF and SDF, other approaches based upon voxel-wise comparison, such as *connectometry*, have been devised [17]. Due to the necessity of coregistering individual scans to a standardized space, this method may not be suitable for comparing cases involving large space-occupying lesions such as tumors. For example, removal of a large tumor may alter structural anatomy to an extent where serial comparison of pre- and-postoperative scans is unfeasible.

### Use of Tractography for Evaluation of Perilesional White Matter: Qualitative Approaches

As primary brain neoplasms possess heterogeneous histopathological characteristics, their growth may be diffuse or intracapsular, may be spread along anatomical planes (e.g., butterfly gliomas), may cause intralesional or perilesional necrosis, or may be associated with significant edema. Each of these factors affects surrounding white matter differently. In general, however, it is observed that benign, non-neuronal lesions such as meningiomas and cavernomas cause tract displacement, whereas diffusely proliferating gliomas produce incremental tract infiltration and destruction with increasing histopathological grade [5, 34–36] (Fig. 1).

Qualitatively, tractography may be used to visualize the displacement, disruption, or infiltration of perilesional white matter. Displacement is defined as a simple shift of white matter trajectories by a lesion that does not otherwise destroy them in any way [37]. Lesions comprised of non-neural tissue, such as metastases or meningiomas, tend to displace white matter rather than specifically damage or destroy it. Though lesions such as cavernomas cause displacement, a pressure effect may damage

neuronal integrity, causing cellular atrophy and loss of diffusion signal. Disruption is therefore defined as breakage or *thinning* of white matter trajectories secondary to a lesion [6]. High-grade gliomas, comprised of aberrant neural tissue, may infiltrate [4, 5] white matter tracts, causing a combination of displacement, disruption, or outright destruction of white matter. Displaced tracts may return to their normal position following lesion removal, with minimal residual deficits. Disrupted tracts, which may appear *thinned* or broken on preoperative tractography, may assume their normal appearance following removal of a lesion exerting pressure upon them. White matter that has been infiltrated by tumor may require sacrifice during surgery, provided it is not eloquent or critical to function.

### Advantages of Using Non-tensor White Matter Imaging Techniques with Structural Lesions

Non-tensor approaches such as GQI are preferable for obtaining qualitative data towards presurgical analysis. Due to the mass effect produced by space-occupying lesions within the cranial vault, intact surrounding white matter pathways may be pushed into deviated trajectories, assuming spatial relationships that are difficult to accurately predict based on anatomical principles. An algorithm with ability to demonstrate crossing trajectories at high resolution may therefore be preferable to demonstrate pathological arrangements or spatial relationship of white matter tracts in a 3-dimensional fashion and in relation to a tumor with mass effect [9, 20, 38]. As the diffusion properties of water within neural tissues are measured during acquisition, the presence of peritumoral edema may affect tractography results. Subsequently, tracts passing through an edematous region may be *falsely* incomplete, may show disruption, or may be terminated abruptly [5, 39]. Zhang et al. [39] demonstrated that GQI-based tractography (i.e., HDFT) was more reliably able to demonstrate robust white matter tracts passing through edematous peritumoral areas compared to DTI. HARDI methods have also shown an ability to trace tracts passing through regions of peritumoral edema [40, 41]. This is an important caveat as surgeons may mistakenly believe that surrounding white matter tracts have been disrupted by tumor when, in fact, they are *artificially* obscured due to edema. In these situations, preoperative tractography is misleading and surgeons may have to rely upon the complementary use of alternative adjuncts such as intraoperative electrical stimulation (IES) [42] to define eloquent white matter and guide resection depth. It is obvious that for tractography to be considered a valid preoperative planning technique, it must provide an accurate representation of close-proximity peritumoral fibers. The visual

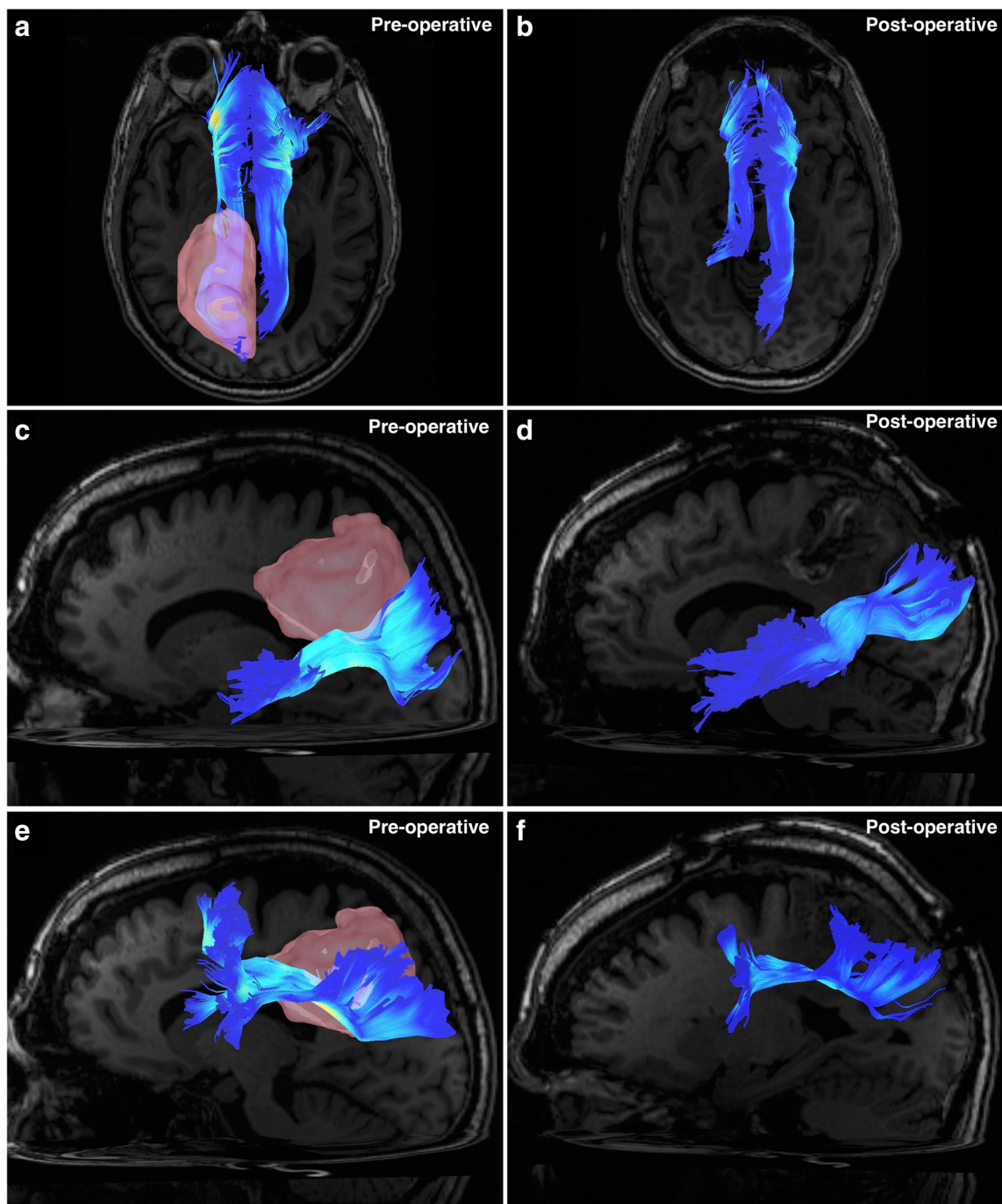


**Fig. 2** All images are taken from the case described in Fig. 1. Tracts have been colored according to an index with darker blue representing lower QA values and white representing high QA values. **(a)** A superior-aspect axial view image demonstrating the left and right cingulum bundles preoperatively. Apparent is the infiltration of the left cingulum by the parietal tumor (pink). **(b)** A superior-aspect axial view image demonstrating the left and right cingulum bundles postoperatively. The posterior aspect of the left cingulum has been sacrificed due to tumor infiltration. **(c)** A left-sided sagittal view demonstrating the left-sided middle longitudinal fasciculus preoperatively. The superior aspect of the fascicle has been infiltrated by the inferior growth of the tumor. **(d)** A left-

sided sagittal view demonstrating the left-sided middle longitudinal fasciculus postoperatively. Apparent is the very slight loss of fibers from the superior margin of the fascicle, sacrificed due to tumor invasion. **(e)** A left-sided sagittal view demonstrating the left-sided superior longitudinal fasciculus preoperatively. The medial boundary of the fascicle abuts the lateral aspect of tumor growth, and these fibers have been infiltrated. **(f)** A left-sided sagittal view demonstrating the left-sided superior longitudinal fasciculus postoperatively. Medial fibers have been sacrificed due to tumor removal, revealing an overall thinning of the bundle

representation of white matter pathways affected by pathological processes is better obtained via advanced white matter imaging techniques, as outlined above (Fig. 2, compare with Fig. 7).

### Approaches to Fiber Tracking

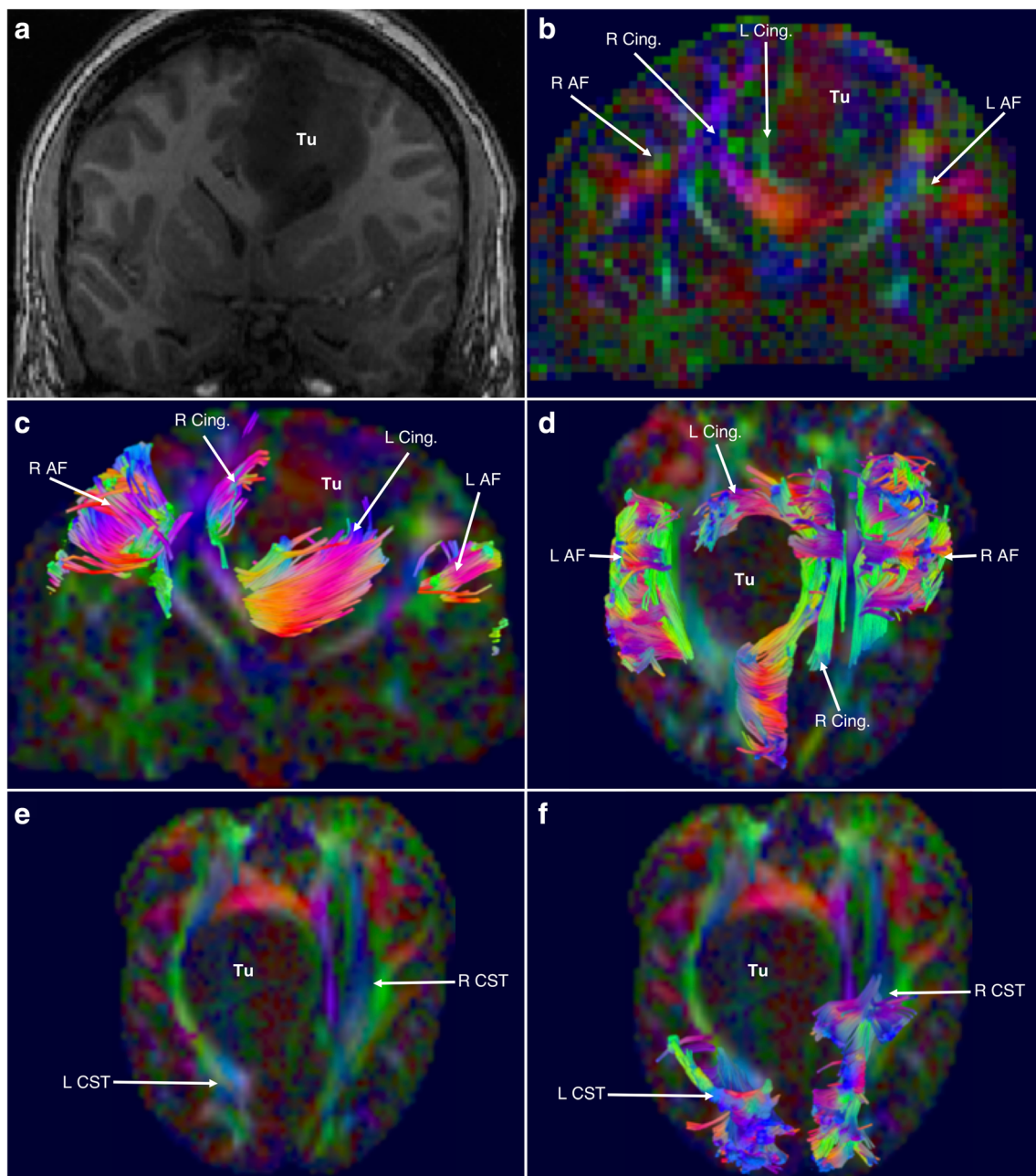
Due to the architectural distortion caused by intraparenchymal lesions, the use of an atlas-based approach [11, 12, 14, 15] to seeding fiber tracts is problematic *versus* fiber tracking in healthy subjects. This is also true for the visualization of very small neural structures such as the cranial nerves [16, 43]. In these situations, manual placement of ROIs is preferable, together with a user's extensive knowledge of radiological and white matter neuroanatomy. As white matter tracts may be displaced, disrupted, or infiltrated by the lesion, ROI placement may also vary from healthy subjects. Other aids may include the use of overlaid structural images, such as T1 or FLAIR sequences, though these do not give an idea of fiber orientation or trajectory. A directional color map of tensor/SDF directionality is useful for ROI placement [44]. Red-green-blue directional encoding provides information regarding either anteroposterior, superoinferior, or horizontal tract directionality, enabling localization. When utilized in conjunction with prior anatomical knowledge, color-encoding schemes are particularly helpful for localizing and seeding deviated tracts within distorted parenchyma (Fig. 3).

### Use of Tractography for Evaluation of Perilesional White Matter: Quantitative Approaches

As qualitative tract visualization may be affected by edema or necrosis, quantitative information contained in the peritumoral voxels (or around other structural lesions) may provide information regarding the integrity of the underlying white matter tracts. By comparing these markers, for example QA, from affected areas in relation to contralateral homologous unaffected regions from the same subject, or across subjects, a quantitative indicator of white matter integrity can be attained with potential for prognostication [4, 5, 17]. Concurrent qualitative tractography or validation of index values is required for meaningful interpretation, thereby leading us to advocate a combined qualitative and quantitative approach while interpreting the data from tractography [4, 5]. DTI has been more prevalent and primarily been utilized for quantitative white matter evaluation in neuro-oncology despite its weaknesses [34, 45–49]. Due to its use of a single tensor per voxel, affected by all fiber orientations

**Fig. 3** A 26-year-old male presented to the emergency department following new-onset, intractable, generalized, tonic-clonic seizures. A large, 7-cm mass was found within the left sensorimotor area. He underwent awake craniotomy with electrical stimulation and microsurgical resection of the tumor. Subtotal resection was achieved due to the tumors' proximity to the motor strip. The postoperative period was otherwise unremarkable, and he was discharged for follow-up. Surgical pathology revealed a WHO grade II glioma with p53, IDH1, and MGMT mutations. **(a)** Anteroposterior view of a coronal T1 slice demonstrating the tumor (Tu) within the left hemisphere, abutting the sensorimotor area. **(b)** Anteroposterior view of the red-green-blue (RGB) SDF color map. Green areas indicate anteroposterior fiber orientation; blue areas indicate superoinferior fiber orientation; red areas indicate horizontal fiber orientation. Tumor is indicated by Tu. On the right, the arcuate (R AF) and cingulum (R Cing.) have been indicated, the arcuate lateral to the corona radiata and the cingulum medial to it, and above the corpus callosum. On the left, the arcuate (L AF) has been displaced laterally and ventrally by the mass, whereas the cingulum (L Cing.) has been displaced medially and ventrally (i.e., towards the contralateral hemisphere). **(c)** Anteroposterior view of the RGB SDF color map. Green areas indicate anteroposterior fiber orientation; blue areas indicate superoinferior fiber orientation; red areas indicate horizontal fiber orientation. Tumor is indicated by Tu. Fiber tracts have been overlaid. From this image, the right arcuate (R AF) and cingulum (R Cing.) are demonstrated relative to the contralateral arcuate (L AF) and cingulum (L Cing.) which have been displaced. The left arcuate has been displaced laterally and ventrally, whereas the anterior fibers of the cingulum have been displaced medially and ventrally and are curving underneath the inferior aspect of the tumor as they travel forward. **(d)** Superoinferior view of the RGB SDF color map. Green areas indicate anteroposterior fiber orientation; blue areas indicate superoinferior fiber orientation; red areas indicate horizontal fiber orientation. Tumor is indicated by Tu. Fiber tracts have been overlaid. From this aspect, the displacement of the left arcuate (L AF) is apparent, as is the highly deviated trajectory of the left cingulum (L Cing.), which curves around the anterior aspect of the tumor. The right cingulum (R Cing.) has been mildly displaced by mass effect, whereas the right arcuate (R AF) is largely intact and nondeviated. **(e)** Superoinferior view of the RGB SDF color map. Green areas indicate anteroposterior fiber orientation; blue areas indicate superoinferior fiber orientation; red areas indicate horizontal fiber orientation. Tumor is indicated by Tu. The course of the corticospinal fiber tracts is indicated, as it passes through the internal capsule. At this level, the left corticospinal tract (L CST) is severely posteriorly displaced, by the tumor, relative to its contralateral counterpart (R CST). **(f)** Superoinferior view of the RGB SDF color map. Green areas indicate anteroposterior fiber orientation; blue areas indicate superoinferior fiber orientation; red areas indicate horizontal fiber orientation. Tumor is indicated by Tu. Fiber tracts have been overlaid. Here, the amount of displacement of the left corticospinal (L CST) tract *versus* the right (R CST) is readily apparent

contained within, heterogeneous fiber populations may exert an effect upon peritumoral index values, possibly confounding interpretation [23, 38, 39, 50]. Non-tensor approaches to quantitative peritumoral white matter analysis have been attempted [4]. Nevertheless, due to the heterogeneous molecular and phenotypic characteristics of gliomas [51] combined with anatomical variables and acquisition considerations previously described, achieving a validated reference index of peritumoral anisotropy is a challenging task requiring extensive work (Fig. 4).



## Interpretation of Indices

Extensive literature regarding the interpretation of quantitative diffusion indices in brain tumor subjects is lacking. Occult infiltration of visually and radiologically normal-appearing (on standard sequences) tissue is particularly challenging to detect [46, 52]. Nevertheless, attempts to correlate measured quantitative index values with underlying change have been made. For example, a DTI-based scheme [34, 53] defined *disruption* as isotropic/near-isotropic FA values, *infiltration* as a reduction of FA by >25% with increased apparent diffusion coefficients (ADCs) and abnormal color hues on a directionally encoded color map, *edematous white matter* as

a reduction of FA by >25% with both increased ADC and normal-appearing directional color encoding, and *displacement* as mildly decreased (<25%) FA values on the affected side *versus* the contralateral side, plus displacement as indicated on directionally encoded color maps. Celtikci et al. [4] studied the non-tensor metrics of white matter displacement caused by low-grade gliomas. They analyzed the QA values of peritumoral tract segments and compared them with whole-tract QA values. Values from the contralateral (unaffected) side were also obtained. The authors found a significant increase in the QA ratio of peritumoral/whole tract segments for affected hemisphere tracts that were visibly displaced. There was a significant decrease in the QA ratio

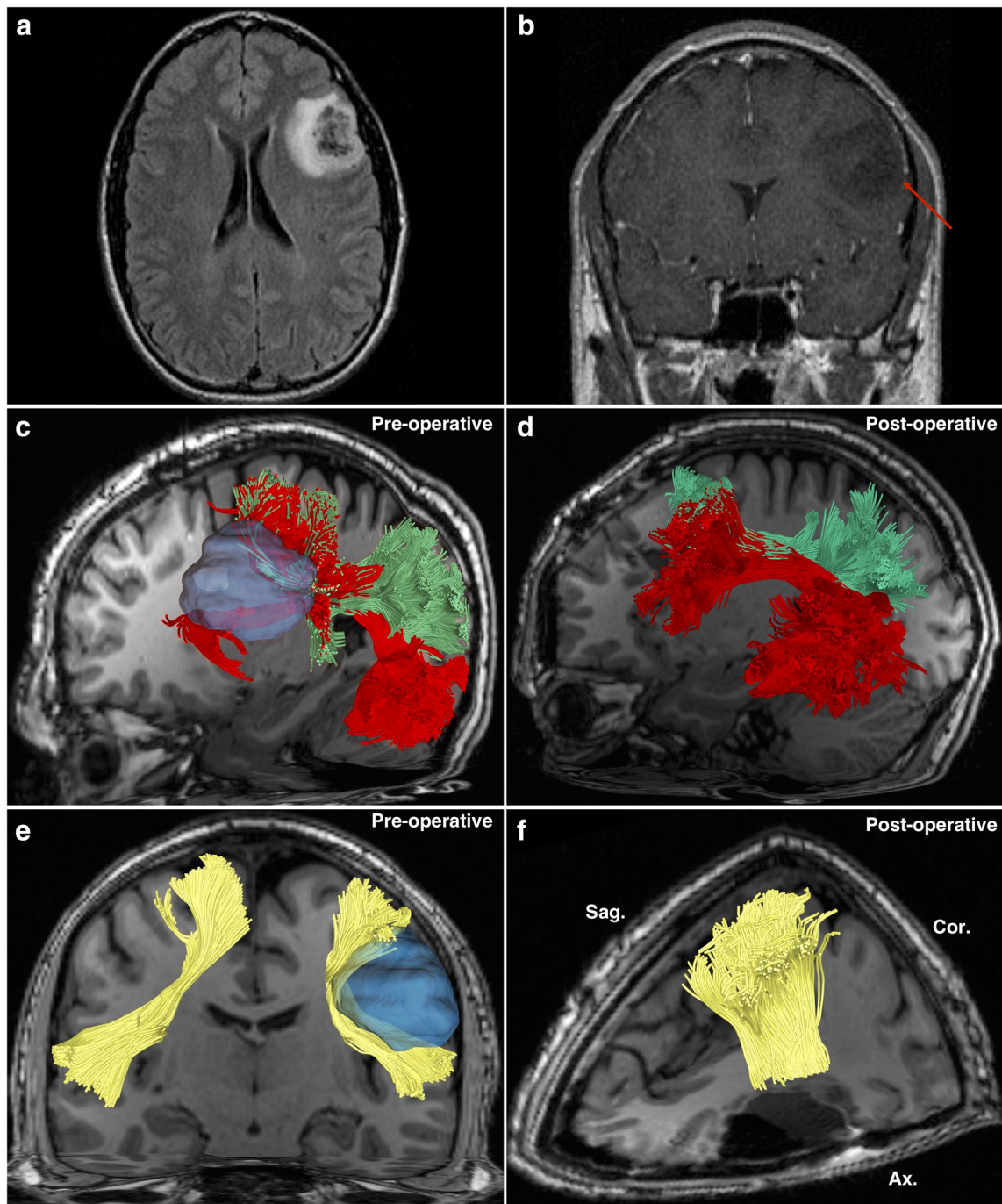


**Fig. 4** A 36-year-old male presented to the outpatient clinic with a history of intermittent seizures and conductive aphasia with intact language comprehension. Investigations revealed a 4-cm lesion in the left inferior frontal lobe in the traditional Broca's area. He underwent craniotomy and subtotal tumor resection under microscopic guidance. Surgical pathology revealed a World Health Organization Grade II astrocytoma with 9P deletion, IDH1 mutation, and MGMT methylation. His postoperative recovery was unremarkable, and he was discharged for routine follow-up. **(a)** A preoperative axial FLAIR sequence image demonstrating the lesion in the left inferior frontal region. **(b)** A preoperative coronal gadolinium-enhanced T1-weighted image demonstrating the tumor in the left inferior frontal region. **(c)** A preoperative oblique-sagittal view of the tumor (blue) and surrounding tracts. The inferior fibers arcuate

fasciculus (AF) in the frontal lobe have been separated from the superior fibers which are intermingled with the fibers of the superior longitudinal fasciculus (green), lying atop the arcuate. **(d)** A postoperative sagittal view of the left hemisphere following tumor removal. Apparent is a more robust collection of arcuate fibers which had been disrupted by the tumor (compare with **(c)**). **(e)** A preoperative coronal view demonstrating specifically the bilateral frontal aslant tracts (yellow). On the left, the tumor (blue) is displacing the middle portion of the frontal aslant tract, giving it a more curved trajectory *versus* its right-sided counterpart. **(f)** A postoperative oblique view demonstrating the resection cavity of the tumor and its relation to the frontal aslant tract (yellow). The very close proximity of the tract to the tumor bed is apparent



of peritumoral/whole tract segments on the affected side for tracts that were visually infiltrated. Though this was a relatively small-volume study of low-grade gliomas in all brain areas, it indicated the potential of the technique as an alternative to FA-based indices.

### Alternative Quantitative Indices

Alternative quantitative indices are available for assessment of perilesional white matter. Acquisition of HDFT scans enables restricted diffusion index (RDI) and non-restricted diffusion index (NRDI) to be obtained in addition to quantitative anisotropy. These indices may be utilized together to enhance an understanding of perilesional white matter changes. For example, areas demonstrating a high RDI can be interpreted as possessing a higher cellular density [54], though these high RDI areas may be isotropic rather than anisotropic. The caveat of this approach is that RDI can demonstrate the presence of perilesional white matter, but due to isotropy, tracts will lack directionality and will appear as *noise* on tractography. Importantly, obtaining RDI and NRDI does not add additional scanning time and is therefore clinically feasible (Fig. 5).

### Predicting Therapeutic Responses

Both qualitative and quantitative tractography approaches have been utilized to predict responses to surgical [55] and nonsurgical [56–59] neuro-oncological interventions. In general, qualitative assessment of white matter replacement on postoperative tractography can give an approximation of functional outcomes [50, 60]. This may be particularly useful for tumors involving the corticospinal tracts or optic radiations, where functional deficits can be readily assessed and correlated with white matter changes. For tumors involving the association fascicles, the neural substrates of abstract faculties such as language, object recognition, and visuospatial localization among many others, correlations between postoperative anatomical tractography and existing or future deficits are harder to make. Moreover, due to edema occurring postoperatively, non-tensor approaches may be of greater benefit for postoperative study, which we have previously discussed. In one of the few large-volume studies in this area, Castellano et al. [55] utilized multimodal data, including qualitative DTI tractography to study the effect of tumor white matter infiltration on surgical outcome in 60 high- and low-grade glioma patients. The authors found that tumor infiltration of certain association tracts and the corticospinal tracts was predictive of suboptimal surgical outcome. This was attributed to the lower likelihood of an infiltrating tumor to be totally resected. As these studies involved primarily DTI-based metrics, it is not

known whether non-tensor approaches may offer similar or improved information pertaining to outcome prediction in glioma cases.

### Combination of Tractography with Diagnostic and Intraoperative Functional Adjuncts: Beyond Structural Imaging

Although tractography is able to demonstrate *in vivo* white matter architecture and cortical connectivity, it does not provide information regarding the function of tracts. Inferences may be made by correlating tract connectivity with known roles of particular cortical areas derived from techniques such as functional MRI (fMRI), magnetoencephalography (MEG), or IES. Holodny et al. [61] first described the technique of fMRI-tractography integration. The authors utilized functional activations corresponding to the motor strip as seeding ROIs for the corticospinal tracts in a series of 7 high-grade glioma patients. The method of using cortical functional activations from either fMRI or MEG as seeding points for tracts underpins the use of these techniques for presurgical planning. As tumors may cause distortion of both gray and white matter anatomy, typical functional areas may become displaced or invaded [62–64]. A combination of functional neuroimaging and white matter tractography therefore reinforces the preoperative benefit of each separate technique by permitting for dedicated anatomo-functional correlation [65–68].

### Intraoperative Electrical Stimulation and Tractography

Application of IES as an operative adjunct guiding resection depth has been well described in the literature [42, 69–71]. Some consider it a *gold standard* method of anatomo-functional correlation due to its ability to provide real-time information pertaining to the eloquence of visualized structures during surgery [72]. Nevertheless, as white matter appears homogeneous to the naked eye, it is impossible to definitively know exactly which structure the probe is stimulating. Furthermore, stimulation may cause propagation of the electrical signal to adjacent areas, eliciting functional response from these structures instead of the area being probed [73]. Regarding the dual use of tractography with IES, the latter method may be useful when considering the inability of DTI to reliably trace fibers through peritumoral areas. Despite *negative* tractography results, IES can demonstrate that these areas, in fact, retain eloquence and necessitate sparing [74]. As non-tensor approaches (i.e., GQI, HARDI) are better able to trace close-proximity peritumoral fiber tracts [39–41],

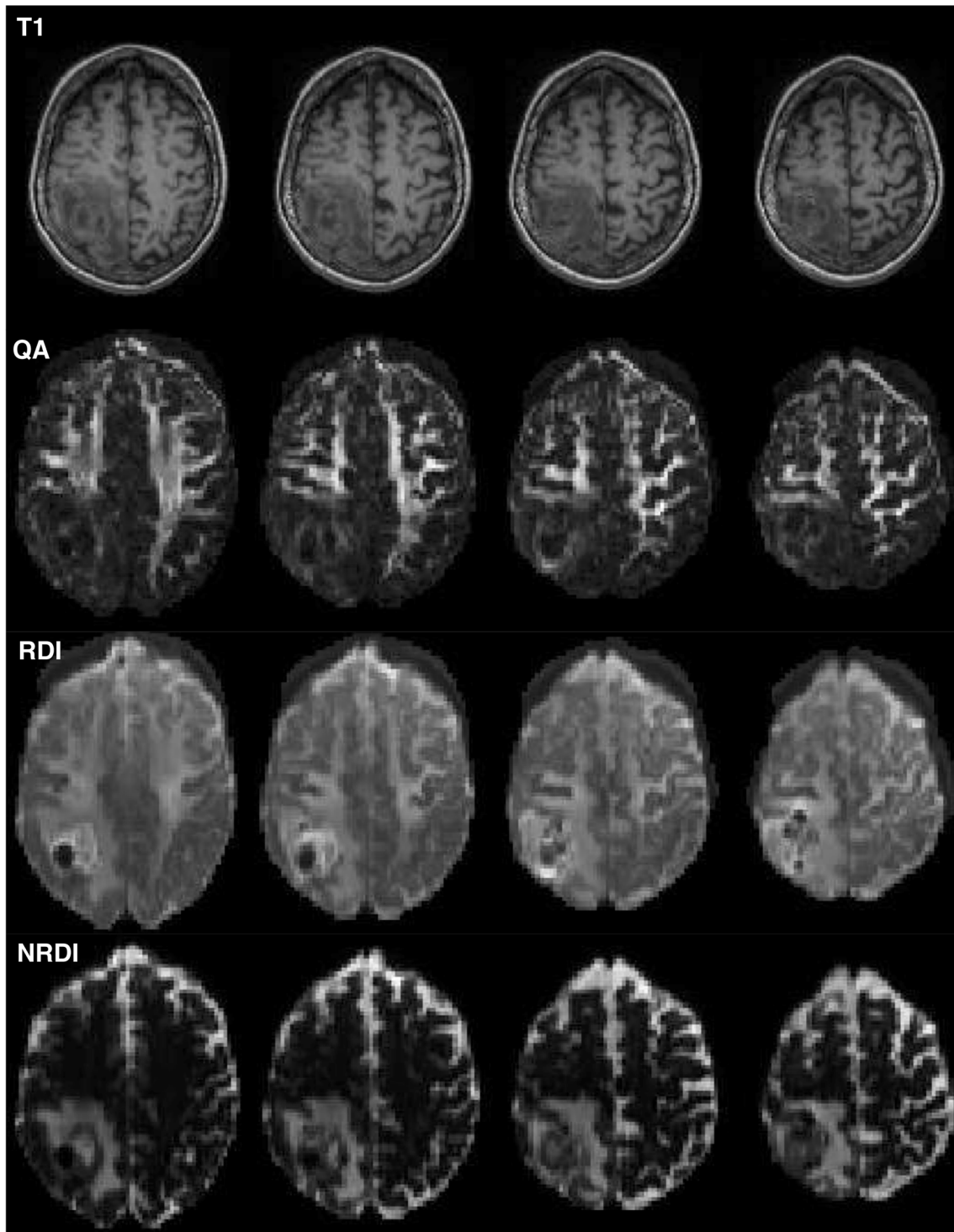


**Fig. 5** The use of alternative indices derived from HDFT scans. On the top row are standard T1-weighted axial slices from a patient with a tumor in the right occipital lobe. Underneath this row are the corresponding slices taken from a QA map. Apparent are the bright areas of higher QA, which correspond to subcortical white matter. Notably in the right occipital lobe, there is an area of very low QA with a loss of white matter definition. The row below this demonstrates the RDI map corresponding

to the same slices as the upper rows. Notably, peritumoral white matter definition is present and superior to the QA map, indicating that tracts may still be passing very close to the tumor, which is not apparent on the QA map. The bottom row is a series of axial slices corresponding to the above, but demonstrating NRDI maps. Apparent on this, and not the others, is the extent of peritumoral edema which may be useful for surgeons in preoperative assessment

combining advanced tractography and IES may lead to an even more accurate method of anato-functional localization. The complementary use of the 2 techniques warrants further exploration.

### Image Guidance and Intraoperative Tractography

Attempts have been made to fuse both preoperative [75, 76] and intraoperative [77, 78] tractography with image guidance methods. Aside from the corticospinal tracts,

this technique may be particularly useful for procedures involving the anterior temporal lobe where Meyer's loop is susceptible to damage due to its proximity to the temporal pole [79, 80]. Preoperative tractography may be of limited benefit for this approach, as MRI sequences are obtained prior to craniotomy and will not account for brain shift occurring upon craniotomy [81]. Upon skull opening, both gray and white matter structures will assume novel spatial position in relation to fixed landmarks, making preoperatively conducted tractography

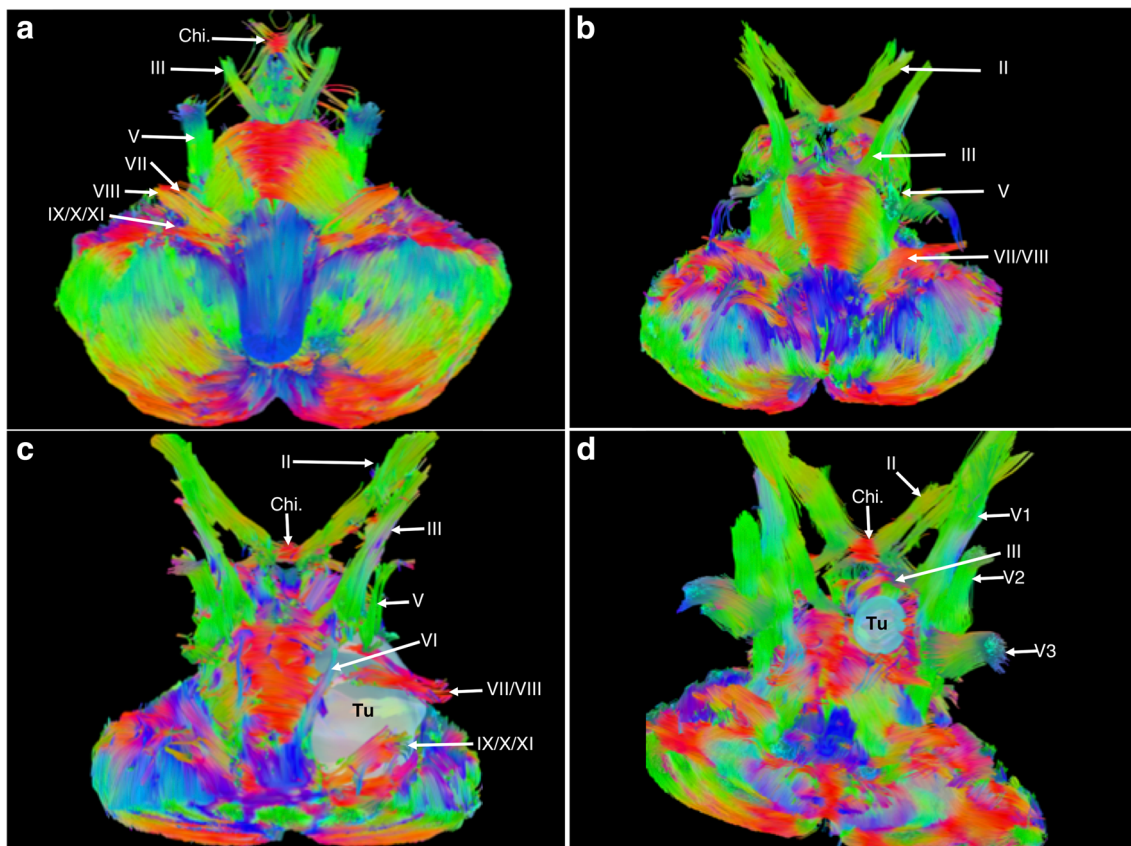


**Fig. 6** (a)–(d) Images obtained by applying GQI-based reconstruction techniques to diffusion data from various healthy and diseased subjects, acquired using various diffusion MRI protocols on various devices. Subjects in (b)–(d) were acquired using a 32-direction diffusion scheme on a Philips device. DSI studio (<http://dsi-studio.labsolver.org>) was utilized for reconstruction and fiber tracking. Color scheme of fibers is directional, with green representing anteroposterior oriented fibers, blue representing superoinferior oriented fibers, and red representing horizontally oriented fibers. After GQI reconstruction, a quantitative anisotropy-based generalized deterministic algorithm was utilized to provide *whole brainstem* reconstruction. This involved only a single ROI, covering the brainstem, cerebellum, and skull base. The maximal fiber turning angle was  $60^\circ$ , the step size was 0.1, the minimal fiber length was 10 mm, and the maximal fiber length was 20 mm. (a) An anterior, oblique, inferosuperior aspect view of the tractographic reconstruction of the brainstem structures of a healthy subject from the Human Connectome Project database (see Panesar et al. [13, 14] for acquisition of parameter details). Visible in a descending order bilaterally are the optic chiasm (Chi.), CN III, CN V, CN VII, CN VIII, and CN IX/X/XI

complex. (b) An anterior, oblique, inferosuperior aspect view of the tractographic reconstruction of the brainstem structures of a healthy subject. Visible in a descending order bilaterally are CN II, CN III, CN V, and CN VII/VIII complex. (c) An anterior, oblique, inferosuperior aspect view of the tractographic reconstruction of the brainstem structures of a subject with a giant (Koos IV) left-sided vestibular schwannoma. The tumor has displaced the CN VII/VIII complex anteriorly and superiorly, while CN V has also been displaced superiorly. CN IX/X/XI has been displaced inferiorly and medially, while CN VI has been displaced medially. The tractography approach was beneficial in preoperative planning and led the surgeons to choose a subtemporal approach to the tumor. (d) An anterior, oblique, inferosuperior aspect view of the tractographic reconstruction of the brainstem structures of a subject with a left-sided petroclival meningioma. CN III has been severely displaced upwards by the tumor, while CN V and VI were in close contact. Also visible from this view are the V1/V2/V3 branches of CN V. The tractography approach was beneficial in preoperative planning and led the surgeons to choose a subtemporal approach to the tumor

nonrepresentative. Feasibility of intraoperative MRI-derived tractography has been demonstrated [77, 78]. As imaging is obtained following craniotomy and

subsequent parenchymal shift, tractography is structurally representative of the novel spatial positioning of white matter. Incorporation of intraoperative tractography

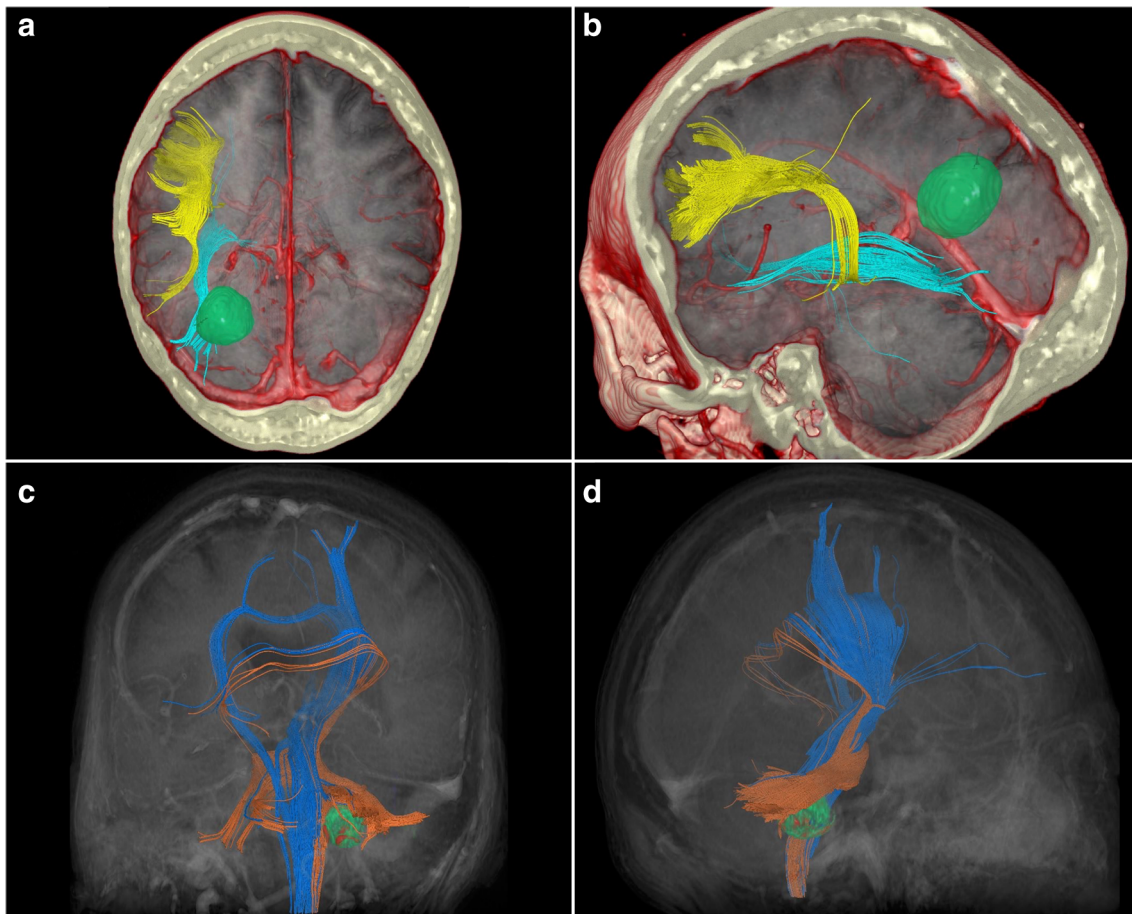


**Fig. 7** (a), (b) A case of a 48-year-old female initially presented with a history of migraine, occipital neuralgia, and left-sided Horner's syndrome, initially diagnosed as a left vertebral artery dissection. This was stented without complication. Two years later, she presented to neurosurgical clinic with left-sided eyelid drooping, sluggish left pupil, left frontoparietal headaches, and generalized clumsiness. Subsequent MRI revealed a 2-cm mass suspicious for glioma. She underwent awake craniotomy with stimulation. The tumor was removed without significant postoperative complication. Surgical pathology revealed a WHO grade IV glioblastoma, with IDH1 R132H mutation. (a) A compound superior-aspect axial slice produced in Surgical Theater (Ohio, USA) virtual reality software demonstrating a combination of computerized tomographic imaging (bone windows and vascular structures) overlaid with T1-weighted MRI images and tractography (obtained via DTI rather than HDFT). Visible in the left occipital lobe is a small glioma with possible displacement of left-sided inferior fronto-occipital fasciculus (blue). This software is compatible with commercially available virtual reality (VR) hardware and was used for preoperative planning for this case. (b) A compound posterior-aspect cutaway view of the left hemisphere produced in Surgical Theater software. Visible from this aspect is the overlying bone of the cranium, vascular structures, parenchyma from a T1-weighted MRI, and inferior fronto-occipital (blue) and arcuate (yellow) fasciculi. What is clear is that no fibers are seen to be in close proximity to the tumor. This may be because of the problems with DTI reconstruction techniques demonstrating close-

proximity fibers. This software is compatible with commercially available VR hardware and was used for preoperative planning for this case. (c), (d) A case of a 66-year-old female was admitted via the emergency department with symptoms including dizziness, diplopia, nystagmus, partial right-sided VI palsy, and intractable nausea. MRI on admission revealed a hemorrhage within the right middle cerebellar peduncle, from a likely cavernous malformation. She underwent stereotactically guided right retromastoid craniotomy, microscopic resection aided by the use of a microscopic CO<sub>2</sub> laser. During surgery, she was found to have hematoma within the right middle cerebellar peduncle, surrounding a 5-mm cavernous malformation. Removal was successful, and she suffered no postoperative complications. (c) A posterior oblique, coronal view using a combination of computerized tomography angiography, T1-weighted MRI, and DTI tractography. Blue fibers represent the bilateral corticospinal tracts, while the orange fibers include those of the middle cerebellar peduncle surrounding the cavernous malformation and possible hematoma. Both the corticospinal tract fibers and middle cerebellar peduncular fibers suffer from false continuity artifacts which are, in fact, corpus callosum fibers. This is a recognized shortcoming of the DTI technique. (d) A right-sided sagittal view using the same imaging sequences described in (c). Clear from this aspect are the orange middle cerebellar peduncular fibers, surrounding the cavernous malformation. The peduncular fibers suffer false continuities with the blue corticospinal tract fibers, while both corticospinal and peduncular fibers falsely blend with fibers of the corpus callosum

sequences with image guidance [77, 78, 81, 82] to guide resection and preserve eloquent white matter may emerge as a potential technique in the future.

### Tractography and Cranial Nerve Reconstruction

One of the biggest challenges in neurosurgical tractography has been the accurate tracking of cranial nerves [16, 43, 83, 84]. Imaging cranial nerve structures is particularly important for the skull base surgeon as they are often displaced by tumors or vascular structures and must be preserved to prevent deficits. Few plain imaging techniques [85, 86] are able to visualize cranial nerve structures reliably due to both their very small size and potential for imaging artifacts conferred by surrounding structures such as bone and air-filled maxillo-facial sinuses. Tractography has been used both qualitatively [16, 83, 84, 87–90] and quantitatively [91–95] for cranial nerve applications. Qualitatively, it may be useful to delineate the optic nerves in gliomas [96], chiasmatic displacement by pituitary tumors [16, 97], the trigeminal nerve in trigeminal neuralgia [90–95], and the vestibulocochlear complex in acoustic schwannomas [16, 87, 90]. Quantitatively, the use of diffusion indices has been trialed to provide an indicator of nerve impingement in trigeminal neuralgia and hemifacial spasm syndromes [91–95].

Despite these potential applications, obtaining reliable, surgically useful tractography of these very small structures remains challenging and optimal acquisition sequences may differ from those used to visualize hemispheric white matter architecture. In our 2016 paper [16], we highlighted a deterministic HDFT approach using user-positioned ROIs, which successfully traced cranial nerves I–XII in 5 healthy and 3 diseased subjects including an optic-hypothalamic glioma, a petroclival meningioma, and a giant adenoma demonstrating suprasellar extension and cavernous sinus invasion. Alternative approaches that have demonstrated promise include the use of DTI in combination with probabilistic tractography [43, 98], and *full brainstem tracking* (see Fig. 6). Future studies should ideally focus upon the correlation of fiber tractography with both intraoperative visual confirmation and neurophysiological monitoring.

### Future Directions

We have highlighted the potential benefits and pitfalls inherent to the neurosurgical application of *in vivo* MRI tractography. Though DTI has had the advantage of being the first available tractography method, it has significant limitations (Fig. 7). Non-tensor approaches, which are able to resolve intravoxel crossing fibers, may be advantageous for qualitative tract visualization in brain tumor cases. Despite initial attempts towards utilizing non-FA metrics for quantitative white matter analysis, further validation is required via

future studies. A validated reference index of QA values pertaining to both healthy and diseased states is required for accurate quantitative analysis while utilizing GQI-based techniques. Some have questioned the value of tractography as a presurgical planning aid [99] given that IES techniques can provide direct functional information. One potential way to address this controversy is to correlate first intraoperative tractography with image guidance for spatial accuracy and then to correlate this data with functional information provided by IES. Further avenues of exploration include the use of tractography as a biomarker in neurodegenerative conditions [17, 100], integrating it with virtual reality modalities (see Fig. 7) and assessing its usefulness in neoplasms of the spinal cord.

### Conclusions

Advanced white matter imaging techniques including HDFT are a valuable method with ability to enhance neurosurgical planning. Addressing controversies pertaining to methodology and application will enable optimization of tractography for neurosurgical planning. As tractography does not offer functional information, further work must be done to integrate it with functional adjuncts such as IES, and other surgical adjuncts such as image guidance. A true, gold standard approach to neuro-oncology cases is therefore a holistic one consisting of both structural and functional adjuncts, and which ultimately translates to optimized patient outcomes.

**Publisher's Note** Springer Nature remains neutral with regard to jurisdictional claims in published maps and institutional affiliations.

### References

- Schmahmann JD, Pandya DN. Cerebral White Matter—Historical Evolution of Facts and Notions Concerning the Organization of the Fiber Pathways of the Brain. *J Hist Neurosci*. 2007;16(3):237–67.
- de Schotten MT, Dell'Acqua F, Valabregue R, Catani M. Monkey to human comparative anatomy of the frontal lobe association tracts. *Cortex*. 2012;48(1):82–96.
- Forkel SJ, de Schotten MT, Kawadler JM, Dell'Acqua F, Danek A, Catani M. The anatomy of fronto-occipital connections from early blunt dissections to contemporary tractography. *Cortex*. 2014;56:73–84.
- Celtikci P, Fernandes-Cabral DT, Yeh F-C, Panesar SS, Fernandez-Miranda JC. Generalized q-sampling imaging fiber tractography reveals displacement and infiltration of fiber tracts in low-grade gliomas. *Neuroradiology*. 2018;60(3):267–80.
- Abhinav K, Yeh F-C, Mansouri A, Zadeh G, Fernandez-Miranda JC. High-definition fiber tractography for the evaluation of perilesional white matter tracts in high-grade glioma surgery. *Neuro-Oncol*. 2015;17(9):1199–209.
- Abhinav K, Pathak S, Richardson RM, Engh J, Gardner P, Yeh F-C, et al. Application of High-Definition Fiber Tractography in the

- Management of Supratentorial Cavernous Malformations: A Combined Qualitative and Quantitative Approach. *Neurosurgery*. 2014;74(6):668–81.
7. Basser PJ, Mattiello J, LeBihan D. MR diffusion tensor spectroscopy and imaging. *Biophys J*. 1994;66(1):259–67.
  8. Farquharson S, Tournier J-D, Calamante F, Fabbini G, Schneider-Kolsky M, Jackson GD, et al. White matter fiber tractography: why we need to move beyond DTI. *J Neurosurg*. 2013;118(6):1367–77.
  9. Fernandez-Miranda JC, Pathak S, Engh J, Jarbo K, Verstynen T, Yeh F-C, et al. High-definition fiber tractography of the human brain: neuroanatomical validation and neurosurgical applications. *Neurosurgery*. 2012;71(2):430–53.
  10. Fernandez-Miranda JC, Engh JA, Pathak SK, Madhok R, Boada FE, Schneider W, et al. High-definition fiber tracking guidance for intraparenchymal endoscopic port surgery. *J Neurosurg*. 2009;113(5):990–9.
  11. Fernández-Miranda JC, Wang Y, Pathak S, Stefaneau L, Verstynen T, Yeh F-C. Asymmetry, connectivity, and segmentation of the arcuate fascicle in the human brain. *Brain Struct Funct*. 2015;220(3):1665–80.
  12. Wang X, Pathak S, Stefaneau L, Yeh F-C, Li S, Fernandez-Miranda JC. Subcomponents and connectivity of the superior longitudinal fasciculus in the human brain. *Brain Struct Funct*. 2016;221(4):2075–92.
  13. Panesar SS, Yeh FC, Deibert CP, Fernandes-Cabral D, Rowthu V, Celtikci P, Celtikci E, Hula WD, Pathak S, Fernández-Miranda JC. A diffusion spectrum imaging-based tractographic study into the anatomical subdivision and cortical connectivity of the ventral external capsule: uncinate and inferior fronto-occipital fascicles. *Neuroradiology*. 2017;59(10):971–87.
  14. Panesar SS, Yeh F-C, Deibert CP, Fernandes-Cabral D, Rowthu V, Celtikci P, et al. A diffusion spectrum imaging-based tractographic study into the anatomical subdivision and cortical connectivity of the ventral external capsule: uncinate and inferior fronto-occipital fascicles. *Neuroradiology*. 2017;59(10):971–87.
  15. Wang Y, Fernández-Miranda JC, Verstynen T, Pathak S, Schneider W, Yeh F-C. Rethinking the role of the middle longitudinal fascicle in language and auditory pathways. *Cereb Cortex N Y N 1991*. 2013 23(10):2347–56.
  16. Yoshino M, Abhinav K, Yeh F-C, Panesar S, Fernandes D, Pathak S, et al. Visualization of Cranial Nerves Using High-Definition Fiber Tractography. *Neurosurgery*. 2016;79(1):146–65.
  17. Abhinav K, Yeh F-C, Pathak S, Suski V, Lacomis D, Friedlander RM, et al. Advanced diffusion MRI fiber tracking in neurosurgical and neurodegenerative disorders and neuroanatomical studies: A review. *Biochim Biophys Acta BBA - Mol Basis Dis*. 2014;1842(11):2286–97.
  18. Yeh F-C, Panesar S, Fernandes D, Meola A, Yoshino M, Fernandez-Miranda JC, et al. Population-averaged atlas of the macroscale human structural connectome and its network topology. *NeuroImage*. 2018;178:57–68.
  19. Stejskal EO, Tanner JE. Spin Diffusion Measurements: Spin Echoes in the Presence of a Time-Dependent Field Gradient. *J Chem Phys*. 1965;42(1):288–92.
  20. Jbabdi S, Behrens TEJ, Smith SM. Crossing fibres in tract-based spatial statistics. *NeuroImage*. 2010;49(1):249–56.
  21. Tuch DS, Reese TG, Wiegell MR, Makris N, Belliveau JW, Wedeen VJ. High angular resolution diffusion imaging reveals intravoxel white matter fiber heterogeneity. *Magn Reson Med*. 48(4):577–82.
  22. Chung H-W, Chou M-C, Chen C-Y. Principles and limitations of computational algorithms in clinical diffusion tensor MR tractography. *AJNR Am J Neuroradiol*. 2011;32(1):3–13.
  23. Alexander AL, Hasan KM, Lazar M, Tsuruda JS, Parker DL. Analysis of partial volume effects in diffusion-tensor MRI. *Magn Reson Med*. 2001;45(5):770–80.
  24. Pasternak O, Sochen N, Gur Y, Intrator N, Assaf Y. Free water elimination and mapping from diffusion MRI. *Magn Reson Med*. 2009;62(3):717–30.
  25. Liu C, Bammer R, Acar B, Moseley ME. Characterizing non-Gaussian diffusion by using generalized diffusion tensors. *Magn Reson Med*. 2004;51(5):924–37.
  26. Alexander DC, Barker GJ, Arridge SR. Detection and modeling of non-Gaussian apparent diffusion coefficient profiles in human brain data. *Magn Reson Med*. 2002;48(2):331–40.
  27. Le Bihan D, Poupon C, Amadon A, Lethimonnier F. Artifacts and pitfalls in diffusion MRI. *J Magn Reson Imaging JMRI*. 2006;24(3):478–88.
  28. Jellison BJ, Field AS, Medow J, Lazar M, Salamat MS, Alexander AL. Diffusion Tensor Imaging of Cerebral White Matter: A Pictorial Review of Physics, Fiber Tract Anatomy, and Tumor Imaging Patterns. *Am J Neuroradiol*. 2004;25(3):356–69.
  29. Yeh F-C, Wedeen VJ, Tseng W-YI. Generalized q-sampling imaging. *IEEE Trans Med Imaging*. 2010;29(9):1626–35.
  30. Wedeen VJ, Wang RP, Schmahmann JD, Benner T, Tseng W-YI, Dai G, et al. Diffusion spectrum magnetic resonance imaging (DSI) tractography of crossing fibers. *Neuroimage*. 2008;41(4):1267–77.
  31. Pierpaoli C, Basser PJ. Toward a quantitative assessment of diffusion anisotropy. *Magn Reson Med*. 1996;36(6):893–906.
  32. Pierpaoli C, Jezzard P, Basser PJ, Barnett A, Di Chiro G. Diffusion tensor MR imaging of the human brain. *Radiology*. 1996;201(3):637–48.
  33. Yeh F-C, Verstynen TD, Wang Y, Fernández-Miranda JC, Tseng W-YI. Deterministic diffusion fiber tracking improved by quantitative anisotropy. *PLoS One*. 2013;8(11):e80713.
  34. Witwer BP, Moftakhar R, Hasan KM, Deshmukh P, Haughton V, Field A, et al. Diffusion-tensor imaging of white matter tracts in patients with cerebral neoplasm. *J Neurosurg*. 2002;97(3):568–75.
  35. Wei CW, Guo G, Mikulis DJ. Tumor effects on cerebral white matter as characterized by diffusion tensor tractography. *Can J Neurol Sci J Can Sci Neurol*. 2007;34(1):62–8.
  36. Faraji AH, Abhinav K, Jarbo K, Yeh F-C, Shin SS, Pathak S, et al. Longitudinal evaluation of corticospinal tract in patients with resected brainstem cavernous malformations using high-definition fiber tractography and diffusion connectometry analysis: preliminary experience. *J Neurosurg*. 2015;123(5):1133–44.
  37. Price SJ, Burnet NG, Donovan T, Green HAL, Peña A, Antoun NM, et al. Diffusion Tensor Imaging of Brain Tumours at 3T: A Potential Tool for Assessing White Matter Tract Invasion? *Clin Radiol*. 2003;58(6):455–62.
  38. Vos SB, Jones DK, Jeurissen B, Viergever MA, Leemans A. The influence of complex white matter architecture on the mean diffusivity in diffusion tensor MRI of the human brain. *NeuroImage*. 2012;59(3):2208–16.
  39. Zhang H, Wang Y, Lu T, Qiu B, Tang Y, Ou S, et al. Differences between generalized q-sampling imaging and diffusion tensor imaging in the preoperative visualization of the nerve fiber tracts within peritumoral edema in brain. *Neurosurgery*. 2013;73(6):1044–53; discussion 1053.
  40. Kuhnt D, Bauer MHA, Sommer J, Merhof D, Nimsky C. Optic Radiation Fiber Tractography in Glioma Patients Based on High Angular Resolution Diffusion Imaging with Compressed Sensing Compared with Diffusion Tensor Imaging—Initial Experience. *PLOS ONE*. 2013;8(7):e70973.
  41. Kuhnt D, Bauer MHA, Egger J, Richter M, Kapur T, Sommer J, et al. Fiber tractography based on diffusion tensor imaging compared with high-angular-resolution diffusion imaging with

- compressed sensing: initial experience. *Neurosurgery*. 2013;72 Suppl 1:165–75.
42. Duffau H, Capelle L, Denvil D, Sichez N, Gatignol P, Taillandier L, et al. Usefulness of intraoperative electrical subcortical mapping during surgery for low-grade gliomas located within eloquent brain regions: functional results in a consecutive series of 103 patients. *J Neurosurg*. 2003;98(4):764–78.
  43. Jacquesson T, Frindel C, Kocevar G, Berhouma M, Jouanneau E, Attyé A, Cotton F. Overcoming challenges of cranial nerve tractography: a targeted review. *Neurosurgery*. Accessed 12 Jul 2018.
  44. Raval A, Schulder M, Kingsley P. NI-66Color coded maps of white matter tracts: NO need for tractography. *Neuro-Oncol*. 2014;16(suppl\_5):v153–v153.
  45. Yu CS, Li KC, Xuan Y, Ji XM, Qin W. Diffusion tensor tractography in patients with cerebral tumors: A helpful technique for neurosurgical planning and postoperative assessment. *Eur J Radiol*. 2005;56(2):197–204.
  46. Price SJ, Peña A, Burnet NG, Jena R, Green HAL, Carpenter TA, et al. Tissue signature characterisation of diffusion tensor abnormalities in cerebral gliomas. *Eur Radiol*. 2004;14(10):1909–17.
  47. Goebell E, Paustenbach S, Vaeterlein O, Ding X-Q, Heese O, Fiehler J, et al. Low-grade and anaplastic gliomas: differences in architecture evaluated with diffusion-tensor MR imaging. *Radiology*. 2006;239(1):217–22.
  48. Talos I-F, Zou KH, Kikinis R, Jolesz FA. Volumetric assessment of tumor infiltration of adjacent white matter based on anatomic MRI and diffusion tensor tractography. *Acad Radiol*. 2007;14(4):431–6.
  49. Delgado AF, Nilsson M, Latini F, Mårtensson J, Zetterling M, Bertsson SG, et al. Preoperative Quantitative MR Tractography Compared with Visual Tract Evaluation in Patients with Neuropathologically Confirmed Gliomas Grades II and III: A Prospective Cohort Study. *Radiol Res Pract*. 2016;2016:7671854.
  50. Lazar M, Alexander AL, Thottakara PJ, Badie B, Field AS. White matter reorganization after surgical resection of brain tumors and vascular malformations. *AJNR Am J Neuroradiol*. 2006;27(6):1258–71.
  51. Louis DN, Perry A, Reifenberger G, Deimling A von, Figarella-Branger D, Cavenee WK, et al. The 2016 World Health Organization Classification of Tumors of the Central Nervous System: a summary. *Acta Neuropathol (Berl)*. 2016;131(6):803–20.
  52. Price SJ, Gillard JH. Imaging biomarkers of brain tumour margin and tumour invasion. *Br J Radiol*. 2011;84(Spec Iss 2):S159–67.
  53. Mori S, Frederiksen K, Zijl PCM van, Stieltjes B, Kraut MA, Solaiyappan M, et al. Brain white matter anatomy of tumor patients evaluated with diffusion tensor imaging. *Ann Neurol*. 2002;51(3):377–80.
  54. Bihan DL. Looking into the functional architecture of the brain with diffusion MRI. *Nat Rev Neurosci*. 2003;4(6):469–80.
  55. Castellano A, Bello L, Michelozzi C, Gallucci M, Fava E, Iadanza A, et al. Role of diffusion tensor magnetic resonance tractography in predicting the extent of resection in glioma surgery. *Neuro-Oncol*. 2012;14(2):192–202.
  56. Moffat BA, Chenevert TL, Lawrence TS, Meyer CR, Johnson TD, Dong Q, et al. Functional diffusion map: A noninvasive MRI biomarker for early stratification of clinical brain tumor response. *Proc Natl Acad Sci*. 2005;102(15):5524–9.
  57. Beppu T, Inoue T, Shibata Y, Yamada N, Kurose A, Ogasawara K, et al. Fractional anisotropy value by diffusion tensor magnetic resonance imaging as a predictor of cell density and proliferation activity of glioblastomas. *Surg Neurol*. 2005;63(1):56–61.
  58. Hamstra DA, Galbán CJ, Meyer CR, Johnson TD, Sundgren PC, Tsien C, et al. Functional diffusion map as an early imaging biomarker for high-grade glioma: correlation with conventional radiologic response and overall survival. *J Clin Oncol Off J Am Soc Clin Oncol*. 2008;26(20):3387–94.
  59. Mardor Y, Roth Y, Ochershvilli A, Spiegelmann R, Tichler T, Daniels D, et al. Pretreatment prediction of brain tumors' response to radiation therapy using high b-value diffusion-weighted MRI. *Neoplasia N Y N*. 2004;6(2):136–42.
  60. Chen X, Weigel D, Ganslandt O, Buchfelder M, Nimsky C. Prediction of visual field deficits by diffusion tensor imaging in temporal lobe epilepsy surgery. *NeuroImage*. 2009;45(2):286–97.
  61. Holodny AI, Ollenschlegler MD, Liu W-C, Schulder M, Kalnin AJ. Identification of the Corticospinal Tracts Achieved Using Blood-oxygen-level-dependent and Diffusion Functional MR Imaging in Patients with Brain Tumors. *Am J Neuroradiol*. 2001;22(1):83–8.
  62. Bartolomei F, Bosma I, Klein M, Baayen JC, Reijneveld JC, Postma TJ, et al. How do brain tumors alter functional connectivity? A magnetoencephalography study. *Ann Neurol*. 2006;59(1):128–38.
  63. Schonberg T, Pianka P, Hendler T, Pasternak O, Assaf Y. Characterization of displaced white matter by brain tumors using combined DTI and fMRI. *NeuroImage*. 2006;30(4):1100–11.
  64. Schiffbauer H, Ferrari P, Rowley HA, Berger MS, Roberts TPL. Functional Activity within Brain Tumors: A Magnetic Source Imaging Study. *Neurosurgery*. 2001;49(6):1313–21.
  65. Gaetz W, Scantlebury N, Widjaja E, Rutka J, Bouffet E, Rockel C, et al. Mapping of the cortical spinal tracts using magnetoencephalography and diffusion tensor tractography in pediatric brain tumor patients. *Childs Nerv Syst*. 2010;26(11):1639–45.
  66. Kamada K, Todo T, Masutani Y, Aoki S, Ino K, et al. Visualization of the frontotemporal language fibers by tractography combined with functional magnetic resonance imaging and magnetoencephalography. *J Neurosurg*. 2007;106(1):90–8.
  67. Berman JI, Berger MS, Chung S, Nagarajan SS, Henry RG. Accuracy of diffusion tensor magnetic resonance imaging tractography assessed using intraoperative subcortical stimulation mapping and magnetic source imaging. *J Neurosurg*. 2007;107(3):488–94.
  68. Bookheimer S. Pre-Surgical Language Mapping with Functional Magnetic Resonance Imaging. *Neuropsychol Rev*. 2007;17(2):145–55.
  69. Duffau H, Gatignol P, Mandonnet E, Capelle L, Taillandier L. Intraoperative subcortical stimulation mapping of language pathways in a consecutive series of 115 patients with Grade II glioma in the left dominant hemisphere. *J Neurosurg*. 2008;109(3):461–71.
  70. Sanaï N, Mirzadeh Z, Berger MS. Functional Outcome after Language Mapping for Glioma Resection. *N Engl J Med*. 2008;358(1):18–27.
  71. Szelényi A, Bello L, Duffau H, Fava E, Feigl GC, Galanda M, et al. Intraoperative electrical stimulation in awake craniotomy: methodological aspects of current practice. *Neurosurg Focus*. 2010;28(2):E7.
  72. Borchers S, Himmelbach M, Logothetis N, Kamath H-O. Direct electrical stimulation of human cortex—the gold standard for mapping brain functions? *Nat Rev Neurosci*. 2012;13(1):63.
  73. Mandonnet E, Winkler PA, Duffau H. Direct electrical stimulation as an input gate into brain functional networks: principles, advantages and limitations. *Acta Neurochir (Wien)*. 2010;152(2):185–93.
  74. Leclercq D, Duffau H, Delmaire C, Capelle L, Gatignol P, Ducros M, et al. Comparison of diffusion tensor imaging tractography of language tracts and intraoperative subcortical stimulations. *J Neurosurg*. 2009;112(3):503–11.
  75. Okada T, Mikuni N, Miki Y, Kikuta K, Urayama S, Hanakawa T, et al. Corticospinal Tract Localization: Integration of Diffusion-Tensor Tractography at 3-T MR Imaging with Intraoperative

- White Matter Stimulation Mapping—Preliminary Results. *Radiology*. 2006;240(3):849–57.
76. Bello L, Gambini A, Castellano A, Carrabba G, Acerbi F, Fava E, et al. Motor and language DTI Fiber Tracking combined with intraoperative subcortical mapping for surgical removal of gliomas. *NeuroImage*. 2008;39(1):369–82.
  77. Nimsky C, Ganslandt O, Hastreiter P, Wang R, Benner T, Sorensen AG, et al. Preoperative and intraoperative diffusion tensor imaging-based fiber tracking in glioma surgery. *Neurosurgery*. 2005;56(1):130–8.
  78. Nimsky C, Ganslandt O, Merhof D, Sorensen AG, Fahlbusch R. Intraoperative visualization of the pyramidal tract by diffusion-tensor-imaging-based fiber tracking. *Neuroimage*. 2006;30(4):1219–29.
  79. Sherbondy AJ, Dougherty RF, Napel S, Wandell BA. Identifying the human optic radiation using diffusion imaging and fiber tractography. *J Vis* 2008;8(10):12–12.
  80. Thudium MO, Campos AR, Urbach H, Clusmann H. The Basal Temporal Approach for Mesial Temporal Surgery: Sparing the Meyer Loop With Navigated Diffusion Tensor Tractography. *Oper Neurosurg*. 2010;67(suppl\_2):ons385–90.
  81. Nimsky C, Ganslandt O, Cerny S, Hastreiter P, Greiner G, Fahlbusch R. Quantification of, Visualization of, and Compensation for Brain Shift Using Intraoperative Magnetic Resonance Imaging. *Neurosurgery*. 2000;47(5):1070–80.
  82. Kuhnt D, Bauer MH, Nimsky C. Brain shift compensation and neurosurgical image fusion using intraoperative MRI: current status and future challenges. *Critical Reviews™ in Biomedical Engineering*. 2012;40(3).
  83. Chen DQ, Quan J, Guha A, Tymianski M, Mikulis D, Hodaie M. Three-Dimensional In Vivo Modeling of Vestibular Schwannomas and Surrounding Cranial Nerves With Diffusion Imaging Tractography. *Neurosurgery*. 2011;68(4):1077–83.
  84. Hodaie M, Quan J, Chen DQ. In Vivo Visualization of Cranial Nerve Pathways in Humans Using Diffusion-Based Tractography. *Neurosurgery*. 2010;66(4):788–96.
  85. Mikami T, Minamida Y, Yamaki T, Koyanagi I, Nonaka T, Houkin K. Cranial nerve assessment in posterior fossa tumors with fast imaging employing steady-state acquisition (FIESTA). *Neurosurg Rev*. 2005;28(4):261–6.
  86. Okumura Y, Suzuki M, Takemura A, Tsujii H, Kawahara K, Matsuura Y, et al. [Visualization of the lower cranial nerves by 3D-FIESTA]. *Nihon Hoshasen Gijutsu Gakkai Zasshi*. 2005;61(2):291–7.
  87. Taoka T, Hirabayashi H, Nakagawa H, Sakamoto M, Myochin K, Hirohashi S, et al. Displacement of the facial nerve course by vestibular schwannoma: preoperative visualization using diffusion tensor tractography. *J Magn Reson Imaging Off J Int Soc Magn Reson Med*. 2006;24(5):1005–10.
  88. Cauley KA, Filippi CG. Diffusion-tensor imaging of small nerve bundles: cranial nerves, peripheral nerves, distal spinal cord, and lumbar nerve roots—clinical applications. *Am J Roentgenol*. 2013;201(2):W326–35.
  89. Wei P-H, Qi Z-G, Chen G, Hu P, Li M-C, Liang J-T, et al. Identification of cranial nerves near large vestibular schwannomas using superselective diffusion tensor tractography: experience with 23 cases. *Acta Neurochir (Wien)*. 2015;157(7):1239–49.
  90. Kakizawa Y, Seguchi T, Kodama K, Ogiwara T, Sasaki T, Goto T, et al. Anatomical study of the trigeminal and facial cranial nerves with the aid of 3.0-tesla magnetic resonance imaging. 2008
  91. Hodaie M, Chen DQ, Quan J, Laperriere N. Tractography delineates microstructural changes in the trigeminal nerve after focal radiosurgery for trigeminal neuralgia. *PLoS One*. 2012;7(3):e32745.
  92. Herweh C, Kress B, Rasche D, Tronnier V, Tröger J, Sartor K, et al. Loss of anisotropy in trigeminal neuralgia revealed by diffusion tensor imaging. *Neurology*. 2007;68(10):776–8.
  93. Leal PRL, Roch JA, Hermier M, Souza MAN, Cristiano-Filho G, Sindou M. Structural abnormalities of the trigeminal root revealed by diffusion tensor imaging in patients with trigeminal neuralgia caused by neurovascular compression: a prospective, double-blind, controlled study. *PAIN®*. 2011;152(10):2357–64.
  94. Lutz J, Linn J, Mehrkens JH, Thon N, Stahl R, Seelos K, et al. Trigeminal neuralgia due to neurovascular compression: high-spatial-resolution diffusion-tensor imaging reveals microstructural neural changes. *Radiology*. 2011;258(2):524–30.
  95. Fujiwara S, Sasaki M, Wada T, Kudo K, Hirooka R, Ishigaki D, et al. High-resolution Diffusion Tensor Imaging for the Detection of Diffusion Abnormalities in the Trigeminal Nerves of Patients with Trigeminal Neuralgia Caused by Neurovascular Compression. *J Neuroimaging*. 2011;21(2):e102–8.
  96. Lober RM, Guzman R, Cheshier SH, Fredrick DR, Edwards MS, Yeom KW. Application of diffusion tensor tractography in pediatric optic pathway glioma. *J Neurosurg Pediatr*. 2012;10(4):273–80.
  97. Anik I, Anik Y, Koc K, Ceylan S, Genc H, Altintas O, et al. Evaluation of early visual recovery in pituitary macroadenomas after endoscopic endonasal transphenoidal surgery: Quantitative assessment with diffusion tensor imaging (DTI). *Acta Neurochir (Wien)*. 2011;153(4):831–42.
  98. Jacquesson T, Frindel C, Cotton F. Diffusion Tensor Imaging Tractography Detecting Isolated Oculomotor Nerve Damage After Traumatic Brain Injury. *World Neurosurg*. 2017;100:707.e5–707.e7.
  99. Duffau H. Diffusion Tensor Imaging Is a Research and Educational Tool, but Not Yet a Clinical Tool. *World Neurosurg*. 2014;82(1):e43–5.
  100. Ciccarelli O, Catani M, Johansen-Berg H, Clark C, Thompson A. Diffusion-based tractography in neurological disorders: concepts, applications, and future developments. *Lancet Neurol*. 2008;7(8):715–27.